Vibrational Spectroscopy of Nitroalkane Chains Using Electron Autodetachment and Ar Predissociation

Holger Schneider,[†] Kristen M. Vogelhuber,[†] Florian Schinle,[†] John F. Stanton,[‡] and J. Mathias Weber*,[†]

JILA, NIST, and Department of Chemistry and Biochemistry, University of Colorado, Boulder, Colorado 80309, and Department of Chemistry and Biochemistry, University of Texas at Austin, 1 University Station A5300, Austin, TX 78712-0165

Received: January 7, 2008; Revised Manuscript Received: June 2, 2008

If the binding energy of an excess electron is lower than some of the vibrational levels of its host anion, vibrational excitation can lead to autodetachment. We use excitation of CH stretching modes in nitroalkane anions (2700−3000 cm^{-1}), where the excess electron is localized predominantly on the NO_2 group. We present data on nitroalkane anions of various chain lengths, showing that this technique is a valid approach to the vibrational spectroscopy of such systems extending to nitroalkane anions at least the size of nitropentane. We compare spectra taken by using vibrational autodetachment with spectra obtained by monitoring Ar evaporation from Ar solvated nitroalkane anions. The spectra of nitromethane and nitroethane are assigned on the basis of ab initio calculations with a detailed analysis of Fermi resonances of CH stretching fundamentals with overtones and combination bands of HCH bending modes.

1. Introduction

Vibrational spectroscopy in concert with quantum chemical calculations is an important way to characterize the structure of ions and to draw conclusions on their interaction with other molecular species as the spectra of bare and solvated ions are compared. For a target of mass-selected ions, it is very hard to use straightforward absorption spectroscopy (i.e., the attenuation of light as it passes through a sample) to obtain an infrared (IR) spectrum because of the low density of mass-selected ion beams (typically $<10^5$ cm^{-3}). Therefore, most IR spectroscopy studies on mass selected ions have utilized photodissociation action spectroscopy. This technique uses either resonant (multi)photon absorption (see, e.g., refs 1–8) to dissociate covalent bonds or the evaporation of weakly bound messenger particles upon photon absorption (typically Ar atoms, see, e.g., refs 9–37).

Methods relying on photodissociation have specific limitations. Photon fluences high enough for most IR multiphoton techniques can usually only be achieved with free electron lasers, requiring large multiuser facilities. Although making experiments with table-top light sources feasible, the attachment of Ar atoms or other messengers often leads to very low parent-ion intensities, decreasing the spectroscopic sensitivity in such experiments.

If the binding energy of an excess electron to a molecule is less than the energy of a certain vibrationally excited state, excitation into that state can lead to vibrational autodetachment (VAD). If the lifetime of the excited anion with respect to VAD is short compared to the experimental time scale, the absorption of a photon leads to the formation of neutral products and free electrons with near-unit efficiency. Although VAD is limited to anions with weakly bound electrons, it can be used for such species as an alternative to Ar predissociation (Ar-PD) or multiphoton techniques, with the advantage that the bare ions are easier to produce and more abundant than the Ar solvated species and that one photon will suffice to detach a weakly bound electron.

Unless there is a direct (i.e., nonstatistical) coupling mechanism between the excited vibrational state and the dissociation or detachment coordinates, both the messenger technique and VAD rely to a large extent on intramolecular vibrational relaxation (IVR). In the context of IVR, the situation of VAD is similar to the use of vibrational predissociation in that the initially excited zero-order bright state is embedded in a continuum of dark states (the dissociation continuum and the electron emission continuum). For Ar evaporation, the energy initially deposited in a vibrational mode of the chromophore ion must be redistributed in order to couple to the Ar motion. For VAD from polyatomic anions, an excited vibrational mode is often not directly coupled to electron emission, and energy needs to be redistributed into a mode that is. There has been a lot of interest in IVR processes in the past several decades. Much progress has been made in the description of IVR in the past 10 years, which has been documented in a number of excellent reviews of the field.[38–56]

The coupling of vibrational energy to electronic motion manifests itself in macroscopic systems, for example, as thermionic emission, described by the Richardson equation.[57] In a molecular description, the coupling of vibrational and electronic motion constitutes a breakdown of the Born−Oppenheimer approximation. Ro-vibrational autodetachment (AD) has first been reported by Lineberger and co-workers,[58] where the excess electron on NH$^-$ was ejected after ro-vibrational excitation of the anion. The VAD approach has not been widely used for spectroscopic purposes, and the only time it has been employed with a (partial) focus on IVR was a few years ago by Johnson and co-workers, in the case of bare and Ar solvated nitromethane anions.[13] This earlier observation of VAD leads to the question whether or not the process is comparably prominent in significantly larger molecules. The molecular size

---

* Corresponding author. E-mail: weberjm@jila.colorado.edu. Fax: ++1-303-492-5235.

[†] University of Colorado.

[‡] University of Texas at Austin.

10.1021/jp800124s CCC: \$40.75

could play a role, because the rate for electron emission will depend on the probability of pooling sufficient amounts of energy in the emission-active modes on the experimental time scale. We note, however, that VAD has recently been used by Mikami and co-workers in an IR spectroscopic study of microsolvated benzonitrile radical anions,[59] making it very unlikely that the size will play a role before reaching very large systems with several tens of atoms, depending, of course, on the time between irradiation and detection in a given experiment.

In the present work, we compare VAD as a spectroscopic method to vibrational Ar predissociation for nitroalkane anions up to nitropentane. Nitroalkanes have been reported to have electron affinities just slightly above 2000 cm^{-1},[60] well below the excitation energies for CH stretching modes, with the excess charge localized mostly on the nitro group. The low electron-binding energy facilitates VAD as well as direct photodetachment in the energy region of the CH stretching fundamentals (2700−3000 cm^{-1}). The absorption bands of the CH stretching vibrations in the hydrocarbon are the zero-order bright states, whereas the nitro group serves as a localized energy acceptor, because the most important vibrational modes coupling the anionic and neutral potential energy surfaces are the NO_2 wagging modes.

2. Experimental Section

Our experimental setup has been described in earlier work.[17,20] In brief, nitroalkane anions are produced in the attachment of slow secondary electrons to nitroalkanes in three-body-collisions

$$CH_3(CH_2)_nNO_2 + e^- + M \rightarrow CH_3(CH_2)_nNO_2^- + M \quad (1)$$

(where M is a collision partner) or through attachment to a cluster containing the nitroalkane under study by using an electron impact plasma generated in a pulsed supersonic expansion. The ions are accelerated and mass-selected in a time-of-flight mass spectrometer (ca. 3.7 keV kinetic energy) and irradiated by nanosecond-pulsed IR radiation from an optical parametric converter (LaserVision). Absorption events followed by electron emission yield fast neutral photoproducts, which impact on a microchannel plate detector located behind a reflectron. We monitor the intensity of neutral photoproducts as we tune the IR light source.

In the same supersonic expansion, Ar solvated nitroalkane anions are generated, which serve as targets for a control experiment, where we measure the IR spectra of the anions under study by evaporation of Ar atoms upon photon absorption (Ar nanomatrix spectroscopy):

$$CH_3(CH_2)_nNO_2^- \cdot Ar_m + h\nu \rightarrow CH_3(CH_2)_nNO_2^- + m\,Ar \quad (2)$$

In this case, we register the intensity of bare anionic fragments as a function of the photon energy. In both approaches, ion signals are normalized to the photon flux from the IR source. For all ions, several individual scans were taken on different days (to ensure reproducibility) and coadded to increase the signal-to-noise ratio.

We calibrate our spectra by determining the wavelength of the signal wave of the optical parametric converter in the near IR by using a fiber optic spectrometer, which in turn is calibrated to the emission lines from an Ar hollow cathode discharge. On the basis of the resolution of the spectrometer in the spectral region in question (ca. 2 cm^{-1}) and the intrinsic bandwidth of the optical parametric converter (ca. 2 cm^{-1}), we conservatively assume our frequency scale to be accurate within 3 cm^{-1}.

3. Calculations

To obtain information on the structures of the anions under study and to guide the assignment of the experimental spectra, we performed density functional theory[61] (DFT) calculations by using the B3-LYP functional,[62,63] as well as calculations based on second-order Møller−Plesset perturbation theory with the resolution-of-identity approximation[64,65] (RI-MP2). These calculations have been performed by using the TURBOMOLE program suite,[66] with TZVPP basis sets[67] for all atoms. Numerical calculations of vibrational spectra were carried out for each stationary point found on the potential surface to confirm that the structures are indeed minima. To compare the simple harmonic approximation spectra obtained this way with the experimental spectra, the CH stretching fundamentals were scaled by a factor of 0.956 to account approximately for anharmonicity.

Aside from the main IR bands in nitromethane, smaller spectroscopic features appear, which cannot be explained by fundamental vibrational transitions. Similarly, in nitroethane and the larger molecular species, a greater number of vibrational features with significant intensity are observed in the CH stretching region than can be rationalized by fundamental CH stretching vibrations. These observations suggest that overtones and combination bands of lower-lying vibrational modes play a role, and higher-level anharmonic calculations are necessary for a more complete assignment. To this end, the coupled-cluster singles and doubles method with a perturbative treatment of triple excitations [CCSD(T)][68] was used in conjunction with a modest atomic natural orbital (ANO) basis set[69] to determine the vibrational levels by using second-order vibrational perturbation theory (VPT2).[70] VPT2 requires the polynomial representations of the potential in normal coordinates to fourth order (quartic force constants) and the dipole operator through third order [Note: The quartic force constants and cubic dipole function coefficients having four and three different indices are not needed in VPT2]; these were generated by using a standard procedure[71] based on analytic second derivatives of CCSD(T).[72] The basis sets used in this work are designated as ANO0 and ANO1 and contain about the same number of contracted functions as the ubiquitous cc-pVDZ and the cc-pVTZ basis sets [Note: The ANO0 basis set is precisely the same size as cc-pVDZ, while the ANO1 set has one contracted *s* function more than cc-pVTZ for first row atoms]. The ANO basis sets, however, have been shown to be quite well-suited for the calculation of vibrational levels, especially when the problem at hand demands the use of a small to modestly sized basis set. These calculations used the Mainz−Austin−Budapest version of ACES II.[73,74]

The vibrational levels of the nitroethane anion were calculated with the GUINEA program,[75] which contains a number of sophisticated tools for recognizing and treating resonance interactions. Ultimately, the energy levels of nitroethane were determined by diagonalizing a twelve-by-twelve effective Hamiltonian in the basis of the five hydrogen stretches, six of the two-quantum CH_2 bending levels, and an additional level that is present as a pseudoresonance. [Note: A pseudoresonance is a term given to cases in which the harmonic levels corresponding to a given state nearly coincide, but in which the deperturbed values are vastly different. This occurs when one of the interacting levels has a strong intrinsic anharmonicity (irrespective of its interaction with the other level) and the other does not. In the present case, $\nu_4 + \nu_{24}$ had to be included for this reason. However, it has virtually no intensity (<0.01 km mol^{-1}) in the diagonalized VPT2+F and HAVPT2+F spectra.]

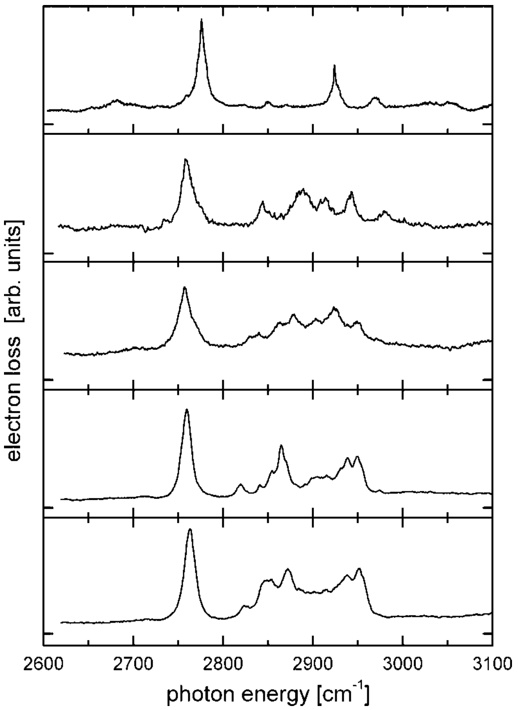

Figure 1. Electron-loss spectra of $CH_3(CH_2)_nNO_2^-$ ($n = 0-4$) upon vibrational excitation in the CH stretching fundamental region.

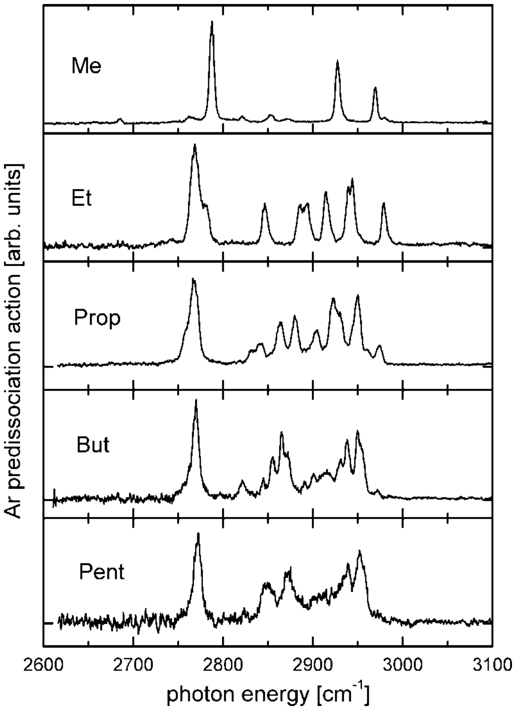

Figure 2. Vibrational Ar-PD spectra of $CH_3(CH_2)_nNO_2^- \cdot Ar_4$ ($n = 0-4$). All Ar atoms are lost upon vibrational excitation.

4. Results and Discussion

4.1. Spectra. Figure 1 displays the IR photodetachment spectra of $CH_3(CH_2)_nNO_2^-$ anions ($n = 0-4$) in the CH stretching region. These neutralization spectra are dominated by resonances which are superimposed on a background of direct photodetachment, which has typically about 25−40% of the cross section of the resonance peaks, depending on the particular molecule under study. Figure 2 shows Ar-PD spectra of $CH_3(CH_2)_nNO_2^- \cdot Ar_4$ ($n = 0-4$). The peaks in these spectra are due to vibrational transitions in the nitroalkane chromophore anion, coupling to the Ar dissociation channel through IVR. We assume the Ar atoms to be located in the general vicinity of the NO_2^- group because of the negative charge localized there. Comparison of the photodetachment and Ar-PD spectra indicates that the resonances in the electron-loss spectra are caused by VAD and that the same vibrational transitions are observed in both cases.

Our results confirm the assumption that VAD can be employed as a tool for vibrational spectroscopy of negative ions of this size range, which can be very useful in cases where other methods, such as Ar-PD, are not possible because of the experimental restrictions of this technique, especially the usually low intensity of the Ar solvated parent ions. The latter effect can be seen immediately in the deteriorating signal-to-noise ratio in the Ar-PD spectra as the vapor pressure of the molecules under study decreases significantly for nitrobutane and nitropentane. Although this effect is noticeable in the Ar-PD spectra, the parent-ion intensity was very high for all bare nitroalkane anions. The small differences in the signal-to-noise ratio in the VAD spectra are due to the fact that the number of individual spectra is not the same for all species.

We do not observe any background in the electron-loss spectra without irradiation, ruling out contributions from the decay of hot metastable parent ions. We cannot make firm statements about the initial ion temperature, but we estimate that the molecules have temperatures on the order of 200−300 K or below. This assumption is based on the fact that we optimized the ion source for production of Ar solvated ions, which are generated in an evaporative ensemble governed by the binding energy of Ar to the anion (ca. 600 cm^{-1})[13] and therefore certainly are below 100 K.

Nitromethane. In the case of nitromethane, the three major transitions observed in the spectra are due to the CH stretching fundamentals of the methyl group, as has been discussed earlier by Johnson and co-workers.[13] Their frequency values and ours agree within the experimental uncertainties of both experiments. The most intense transition among these at 2787 cm^{-1} in the Ar-PD spectrum (2776 cm^{-1} in VAD) is mainly carried by the vibration of the CH group syn to the NO_2^- group. The two other major peaks in the nitromethane spectrum at 2925 and 2969 cm^{-1} are due to the symmetric and antisymmetric CH_2 stretching modes of the two CH groups that are anti to the NO_2^- group. The mode at 2787 cm^{-1} is very strongly red-shifted from the modes in neutral nitromethane because of the interaction of the CH group with the p orbital on the nitrogen atom and corresponding leaking of electron density into the σ^* orbital of that CH bond. This is a general feature in all the nitroalkane anion spectra: the most red-shifted transitions, which are also the most intense features in the spectra, always can be assigned to a localized vibrational mode involving the CH group closest to the nitro group. As a consequence of the Ar atoms being localized close to the negative charge (i.e., at the nitro group), this intense feature at low transition energies is the signature of the CH stretching fundamental that is most strongly influenced by Ar solvation. This is due to the reduction of the electron density leaking into the σ^* antibonding orbital of the corresponding CH bond, which leads to a blue-shift of this mode relative to the bare anion with increasing Ar solvation. The average difference between the peak maxima of this mode in the VAD spectra compared to the Ar-PD spectra is 10 ± 1.1 cm^{-1} for solvation by four Ar atoms (compare Figures 1 and 2). The average blue-shift is therefore +2.5 cm^{-1} per Ar atom for all nitroalkanes under study, consistent with the value previously observed for nitromethane[13] and corroborating our

TABLE 1: Calculated CCSD(T) and Experimental (Ar-PD) Vibrational Levels in the Spectrum of $CH_3NO_2^-$ in cm^{-1a}

mode	Harm ANO1	Harm ANO0	VPT2 ANO0	VPT2 ANO1	VPT2+F ANO0	VPT2+F ANO1	HAVPT2+F	exp.
2 ν_6 (CH_3 umbrella)	2760	2765	2666(1)	2663(1)	2659(4)	2656(5)	2656(5)	2682
$\nu_5 + \nu_6$	2847	2863	2775(0)	2756(0)	2774(6)	2755(5)	2755(4)	2761
ν_3 (CH stretching)	2962	2974	2744^b	3160^b	2810(75)	2798(78)	2799(79)	2787
2 ν_5 (CH_2 bending)	2934	2962	2847(94)	2820(18)	2852(22)	2822(19)	2825(16)	2821
$\nu_4 + \nu_5$	***2947***	***2972***	***2875(2)***	***2826(2)***	***2868(8)***	***2823(3)***	***2825(2)***	
Mixed (see text)					2830(6)	2867(9)	2867(9)	2853
2 ν_4	2960	2982	2975^b	2477^b	2894(16)	2884(8)	2885(8)	2871
ν_2 (sym CH_2 stretch)	3059	3067	2912(79)	2903(80)	2926(62)	2912(46)	2925(73)	2925
***ν_1 (asym CH_2* stretch)**	***3105***	***3112***	***2952(59)***	***2944(59)***	***2959(52)***	***2947(57)***	***2969(58)***	***2969***

[a] The only case where the difference between the peak positions in the VAD and Ar-PD spectra due to Ar solvation was greater than our experimental accuracy (3 cm^{-1}) was ν_3, where the corresponding level in the VAD spectrum is at 2776 cm^{-1}. Calculated intensities (in km mol^{-1}) are in parenthesis. Theoretical values are obtained from second-order vibrational perturbation theory (VPT2) and deperturbation and diagonalization of effective Hamiltonians in the basis discussed in the text (VPT2+F) with both the ANO0 and ANO1 harmonics with the ANO0 anharmonic force field. HAVPT2+F calculations used ANO1 harmonic frequencies for all modes except ν_1 and $\nu_{2,}$ which were adjusted to fit the corresponding experimental fundamentals. Bold italics are used for a'' levels; all others have a' symmetry. All calculated energies are for the bare molecule. [b] >1000 km mol^{-1} (artifacts of close zero-order resonance, as seen in corresponding harmonic frequencies).

earlier assumption that the Ar solvation takes place predominantly at the nitro group.

Aside from the intense CH stretching fundamental bands in the nitromethane Ar-PD and VAD spectra, which are easy to assign even with moderate theoretical effort, there are weaker bands that can tentatively be assigned by high-level anharmonic calculations to overtones and combination bands of HCH bending modes. The principal resonances operative in this anion are between the overtones of the ν_4 and ν_5 bending modes and the red-shifted ν_3 fundamental, all of which have *a*' symmetry. The situation, as it turns out, is quite complicated because there are quite substantial zero-order resonances between ν_4 and $\nu_{10} + \nu_{14}$ as well as between ν_{11} and $2\nu_{14}$. As a result, the *a*' block of an effective Hamiltonian necessitated by the Fermi coupling included the following states in the basis: ν_2, ν_3, $2\nu_4$, $2\nu_5$, $2\nu_6$, $\nu_5 + \nu_6$, $\nu_4 + \nu_{10} + \nu_{14}$, $2\nu_{10} + 2\nu_{14}$, and $2\nu_{10} + \nu_{11}$. Unfortunately, using a simpler basis comprising only fundamentals and two-quantum bending levels, as done for the nitroethane anion (see below) was not adequate for nitromethane, because the peak seen in the spectrum near 2850 cm^{-1} did not appear in the effective Hamiltonian spectrum without the addition of the states necessitated by the two aforementioned resonances.

Table 1 shows results obtained by three different anharmonic calculations: (a) straightforward VPT2 by using the ANO0 anharmonic force fields with both the ANO0 and ANO1 harmonic frequencies, (b) diagonalization of the effective Hamiltonian discussed above and another (a'' block) including ν_2, $\nu_4 + \nu_5$, and $\nu_4 + \nu_6$, and (c) same as (b), except that the ANO1 harmonic force field was adjusted for the (weakly interacting) ν_1 and ν_2 fundamentals in order to bring them into agreement with the observed level positions. The best calculation (HAVPT2+F) is compared to the experiment in Figure 4. The agreement is certainly not quantitative, but the following assignments seem plausible: the two peaks to the red of the 2787 cm^{-1} ν_3 fundamental are straightforwardly assigned to $2\nu_6$ and $\nu_5 + \nu_6$, and the feature at 2821 cm^{-1} is assigned to $2\nu_{5.}$ All bands involving ν_4 are complicated by the secondary resonances $\nu_4 \sim \nu_{10} + \nu_{14}$ and $2\nu_{14} \sim \nu_{11}$, and the states obtained by diagonalization of the effective Hamiltonian involve appreciable mixing with the three- and four-quantum levels. However, the strongest predicted levels at energies higher than $2\nu_5$ are at 2867 cm^{-1} (8.8 km mol^{-1}) and 2885 cm^{-1} (8.0 km mol^{-1}). The dominant elements in the corresponding eigenvectors are $2\nu_4$ and $2\nu_{10} + \nu_{11}$ (essentially 50:50) in the lower-energy feature and the same two dressed basis states (about 60:40, with a different phase relationship) for the higher-energy feature. These states are heavily mixed, however; a more detailed and confident assignment of these small features is an appropriate topic for future study.

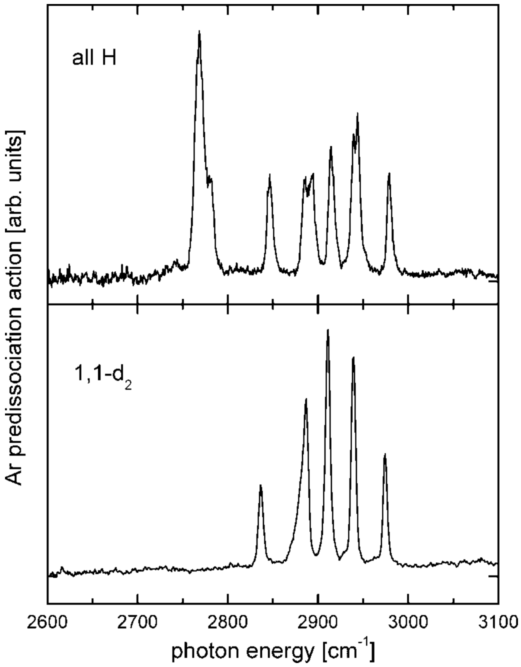

Figure 3. Best calculated spectrum (HAVPT2+F, see Table 1) for $CH_3NO_2^-$ (bottom trace) in comparison with the experimental Ar-PD spectrum (top trace). See Section 3 for details.

It should be pointed out that the most logical assignment, in the absence of the calculations, would have been to associate the three features between ν_1 and ν_3 to the two overtones $2\nu_4$ and $2\nu_5$ as well as $\nu_4 + \nu_5$. This does not appear to be the case, however, because the combination level has a'' symmetry and can interact only with the highest frequency fundamental. The VPT2+F calculations predict an intensity of only 1.5 km mol^{-1} for this transition and an energy of 2825 cm^{-1}.

Nitroethane. The nitromethane spectrum discussed above exhibits three intense bands that can clearly be attributed to the CH stretching fundamentals. The spectrum of nitroethane is significantly more difficult to interpret at first glance, because the number of intense bands is greater than the number of fundamental CH stretching modes. This suggests strong interactions of the CH stretching fundamentals with HCH bending overtones and combination bands, which already lead to weak

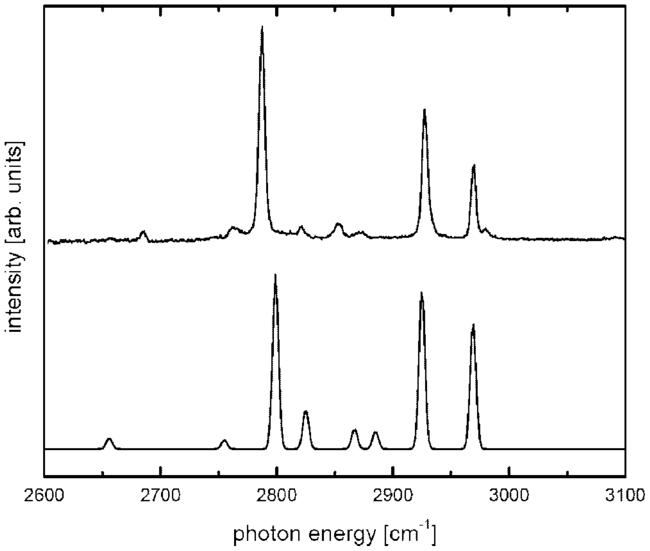

Figure 4. Top: vibrational Ar-PD spectrum of $CH_3CH_2NO_2^-\cdot Ar_4$; bottom: vibrational Ar-PD spectrum of $CH_3CD_2NO_2^-$.

bands in the case of nitromethane (see above). In an attempt to simplify the experimental spectrum and help assignment, we recorded vibrational spectra of $CH_3CD_2NO_2^-$, that is, nitroethane where only the terminal methyl group is hydrogenated (see Figure 3). Deuteration in two positions eliminates two CH stretching fundamentals from the CH stretching region of the nitroethane spectrum, shifting them out of the tuning range of our light source. One of these modes should be the lowest energy band, as described above, and it is indeed missing from the $CH_3CD_2NO_2^-$ spectrum. Interestingly, five intense absorption features remain, although only three CH groups are present. However, the feature at 2846 cm^{-1} shifts upon deuteration by 10 cm^{-1} to lower frequencies, the doublet at ~2890 cm^{-1} with equally intense lines changes into a pair with a dominant component at 2889 cm^{-1} and a shoulder at 2882 cm^{-1}, and the split band at 2940 cm^{-1} is now a single line at 2939 cm^{-1}.

In order to assign the observed IR bands, we performed anharmonic ab initio calculations. The inadequacy of simple VPT2 for this problem is manifest in the results listed in Table 2 and shown in Figure 5, because rather strong harmonic Fermi resonances (particularly between $2\nu_7$ and the red-shifted ν_5 CH stretching level as well as those mixing the overtones $2\nu_6$ and $2\nu_8$ with the ν_4 fundamental) lead to spuriously large intensities and anharmonic shifts involving these levels. When the effective Hamiltonian involving the two-quantum band levels from ν_6 through ν_8 and the five stretching fundamentals is constructed and diagonalized, the levels mentioned above, and, more importantly, the corresponding intensities, are profoundly affected. The corresponding results, denoted as VPT2+F in the table, are in quite respectable qualitative accord with the experimental spectrum, as discussed in the next paragraph. The ANO0 basis set generally gives harmonic frequencies of methyl band levels within 10 cm^{-1} but can be off by ~20 cm^{-1} for stretching levels (see, e.g., refs 76). In the course of this research, the effects of small changes in the harmonic frequencies were explored, and it was found that a remarkably good agreement with the experimental spectrum is obtained when the harmonic levels are shifted within these plausible error ranges. The corresponding harmonically adjusted VPT2[70] levels are also shown in Table 2.

The assignment of the nitroethane anion spectrum is as follows. The high-frequency band at 2979 cm^{-1} is unquestionably ν_1. The pair of lines at 2944 and 2940 cm^{-1} are assigned to $2\nu_6$ and the methylene stretching level ν_3. This assignment is consistent with the disappearance of one component of this doublet in the isotopic spectrum of $CH_3CD_2NO_2^-$. There are two levels that can be assigned to the 2913 cm^{-1} feature: the methyl stretch ν_2 or the combination level $\nu_6 + \nu_7$, although the predicted HAVPT2+F intensity of the fundamental level is greater by an order of magnitude. This is again supported by the persistence of this band in the spectrum of the deuterated compound and what appears to be the loss of a shoulder associated with the dominant transition. Three levels can be associated with the complex apparent doublet at 2885 and 2893 cm^{-1}, all of which are two-quantum levels involving the methyl bending ν_8 fundamental: $2\nu_8$, $\nu_6 + \nu_8$, and $\nu_7 + \nu_8$. The latter is predicted to be the second-strongest absorption, and the shift

TABLE 2: Calculated (CCSD(T)/ANO0 basis) and Experimental Ar-PD Vibrational Modes of $CH_3CH_2NO_2^-$ (Lowest-Energy Esomer, Et-1) in cm^{-1}[a]

mode	harmonic	VPT2	VPT2+F	HAVPT2+F	experimental
ν_5	***2963***	**2754(131)**	**2792(73)**	**2771(74)**	**2769**
ν_4	3019	2870(45)	2840(51)	2842(51)	2846
ν_3	***3077***	**2927(53)**	**2940(40)**	**2943(32)**	**2940**
ν_2	3093	2944(91)	2928(71)	2919(92)	2913
ν_1	3151	2994(50)	2999(41)	2980(39)	2979
$2\nu_6$	3031	2964(280)	2960(48)	2946(49)	2944
$2\nu_7$	***2977***	***2926(243)***	***2884(7)***	***2890(5)***	
$2\nu_8$	2960	2851(67)	2894(31)	2889(31)	2893
$\nu_6 + \nu_7$	***3004***	**2916(17)**	**2916(20)**	**2915(9)**	**2913**
$\nu_7 + \nu_8$	***2969***	**2883(68)**	**2875(13)**	**2880(12)**	**2885**
$\nu_6 + \nu_8$	2996	2904(3)	2903(7)	2896(7)	2893

[a] The only case where the difference between the peak values in the VAD and Ar-PD spectra due to Ar solvation was greater than our experimental accuracy (3 cm^{-1}) was ν_5, where the VAD spectrum exhibits a shift to 2756 cm^{-1}. Levels marked in bold italics involve normal modes that are localized on the methylene fragment and will not appear in the spectrum of $CH_3CD_2NO_2^-$. Intensities (in km mol^{-1}) are given in parenthesis. See text for a discussion of the VPT2, VPT2+F, and HAVPT2+F methods. All calculated energies are for the bare molecule.

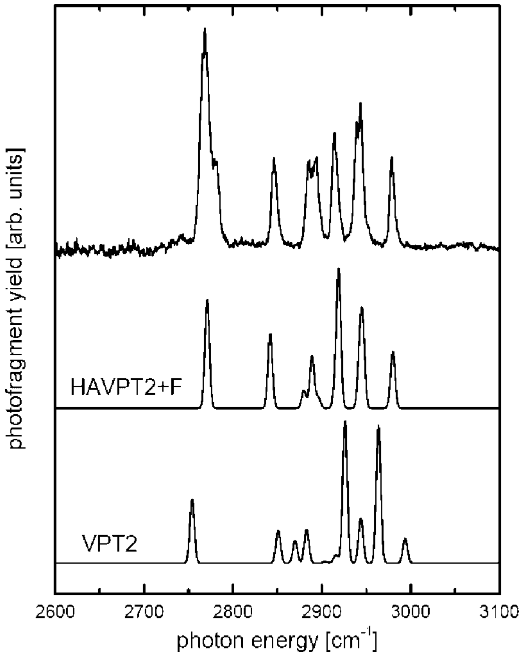

Figure 5. Calculated spectra (lower traces) for $CH_3CH_2NO_2^-$ in comparison with the experimental Ar-PD spectrum (top trace); see Table 2 and Section 3 for details.

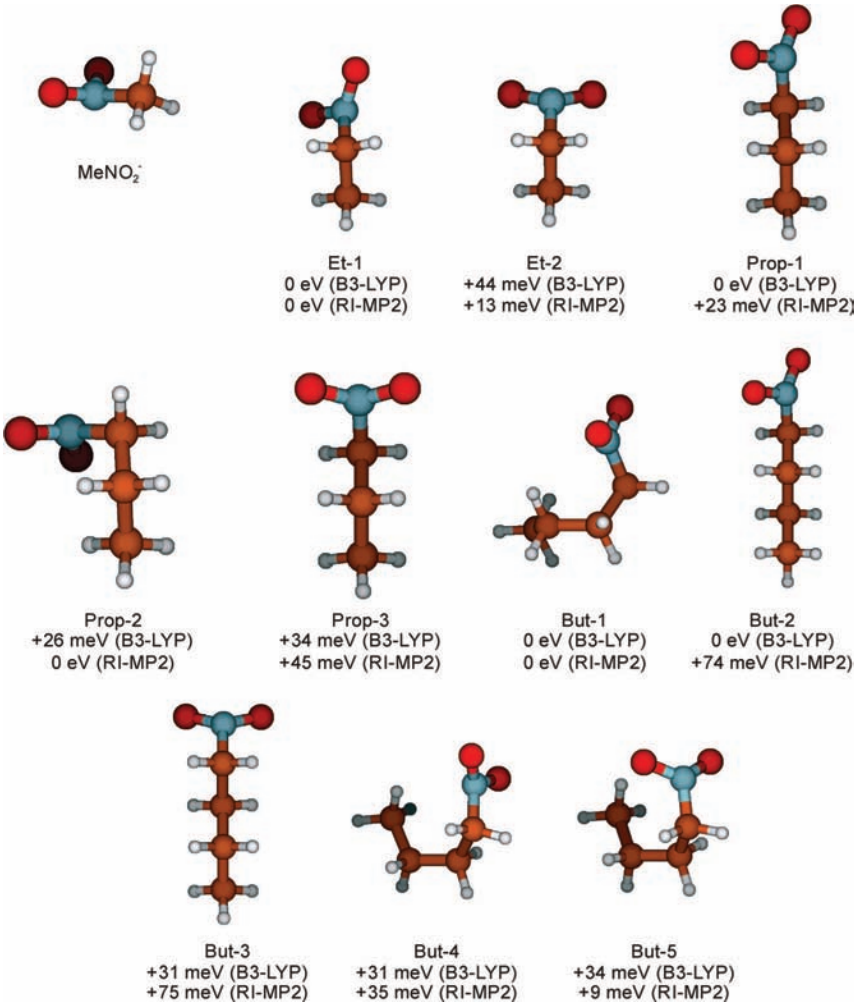

Figure 6. Structural isomers of $CH_3(CH_2)_nNO_2^-$ ($n = 0-3$) and their zero-point corrected relative electronic energies.

of this level out of the window of observation in the isotopic spectrum is consistent with the change in shape of this feature seen experimentally. It now has the appearance of a dominant transition (presumably the overtone of ν_8) broadened by a weaker persistent feature ($\nu_6 + \nu_8$). Assignment of the features at 2846 and 2756 to ν_4 and ν_5 is entirely straightforward and obvious. As demonstrated in this discussion, we are able to unambiguously trace all bands in the nitroethane spectrum to CH stretching fundamentals and HCH overtones and combination bands, and our assignments are consistent with the behavior of the bands in the deuterated spectrum.

One could raise the argument that the complexity in the spectrum of nitroethane could, in principle, be due to the population of different isomers in our beam. In our DFT and MP2 calculations, we found two low-lying isomers for nitroethane (see Figure 6); all other possible isomers generated by rotation about CC bands were found to converge to these two isomers or their enantiomers. However, the close similarity of the Ar-PD and VAD spectra would suggest that the higher energy isomers would be similarly populated in both the bare and the Ar solvated species, which is highly unlikely because of the much lower temperature of the latter. In addition, judging from the harmonic approximation spectra shown in Figure 7, only the calculated spectrum of isomer Et-1 is compatible with the observed spectrum, because the intense low-energy absorption is missing in the calculated spectrum for Et-2. Finally, the anharmonic calculations discussed above appear to completely explain the observed spectrum, and we therefore did not perform an anharmonic calculation on Et-2.

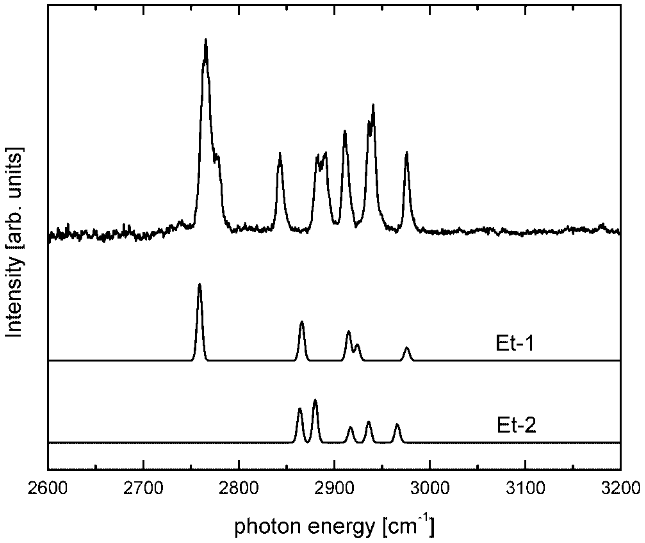

Figure 7. Calculated spectra (B3-LYP, TZVPP basis set, scaled harmonic frequencies) of nitroethane isomers Et-1 and Et-2 (see Figure 6 for nomenclature) compared to the experimental Ar-PD spectrum.

Nitropropane. In the spectra of the larger nitroalkanes, the number of intense absorption bands in the CH stretching region is again consistently greater than the number of CH stretching fundamentals. As discussed for nitroethane, this could in

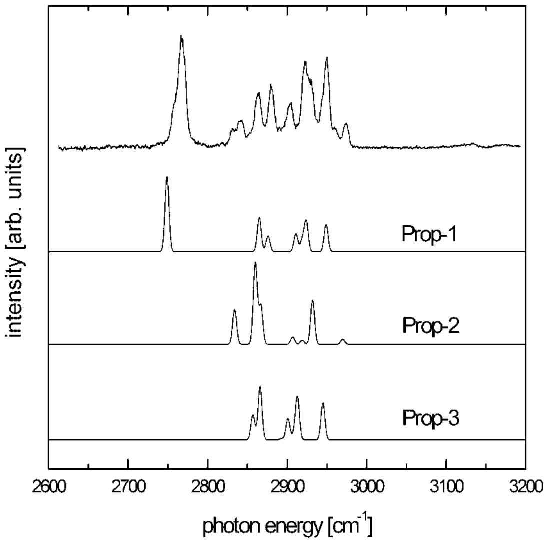

Figure 8. Calculated spectra (B3-LYP, TZVPP basis set, scaled harmonic frequencies) of nitropropane isomers Prop-1, Prop-2, and Prop-3 (see Figure 6 for nomenclature) compared to the experimental Ar-PD spectrum.

principle be rationalized by assuming that more than one isomer could be populated in our ion beam. However, the close similarity of the Ar-PD spectra and the VAD spectra would imply that the bare and Ar solvated species largely have the same populations in various isomers. This is unlikely, especially for the shorter alkanes, because the Ar solvated ions are expected to be much colder than the bare ions.

Nonetheless, we performed DFT and RI-MP2 calculations on all isomers of nitropropane that can be generated by rotations around the CC bonds. Most of these isomers converged into the structures shown in Figure 6. A few others converged into structures that were considerably higher in energy than these low-lying isomers (more than 100 meV) and were discarded. Unfortunately, B3-LYP and RI-MP2 suggest different isomers as the lowest-lying species. The IR spectrum of the RI-MP2 favored isomer Prop-2, however, is incompatible with the intense lowest-energy feature of the IR spectrum at ~2760 cm^{-1} (see Figure 8). This leads us to believe that Prop-1 is most likely the ground-state isomer and is probably the only isomer significantly populated in our ion beam.

In light of the bending modes and Fermi interactions observed and assigned in the nitromethane and nitroethane spectra, this suggests that overtones and/or combination bands of lower lying vibrational modes and their Fermi resonances with the more intense CH stretching fundamental modes lead to complications in the spectrum. We did not perform anharmonic calculations on nitropropane or indeed any of the longer alkane chains because of the increased spectral congestion, the high cost of expensive deuterated target molecules for isotopic labeling experiments, and the high computational cost of anharmonic calculations.

Nitrobutane and Nitropentane. Our calculations for ButNO$_2^-$ indicate that electrostatic interaction between the terminal NO$_2^-$ and CH$_3$ groups leads to the existence of low-lying ring-like structures. As for nitropropane, we performed an extensive isomer search by using structures rotated around the CC bonds as starting geometries. Most of these starting geometries converged into the low-lying isomers shown in Figure 6 or their enantiomers. Some ended in structures more 100 meV above the calculated ground state, which we discarded. In general, the cases of nitrobutane and nitropentane seem less clear than the shorter nitroalkanes because of more significant spectral congestion and lower signal-to-noise ratio in the Ar solvated spectra. Moreover, the energy difference between the lowest-energy isomers is much smaller for the longer-chained species. We therefore refrain from assigning the observed spectral features to particular isomers or vibrational modes, with the exception of the respective lowest energy bands, which seem to be a general feature of nitroalkane anion spectra, and can likely be assigned to a vibration of the CH group closest to the nitro group in all cases.

Given the difficulties associated with the large number of possible starting geometries, we did not perform calculations on nitropentane. It is reasonable to assume, however, that intramolecular ring formation due to H bonding between the terminal nitro and methyl groups will also occur in nitropentane and larger nitroalkane species.

4.2. Remarks on the Mechanism of VAD.

Because the electronic structure of ground-state nitroalkanes does not include electrons that are delocalized along the chain, it is a straightforward assumption that the electron affinities of all nitroalkanes will be similar. Recent photoelectron spectroscopy results for nitroethane anions by Bowen and co-workers[77] support this assumption.

The mechanism for VAD in nitroalkanes has not been elucidated in detail, but one can try to offer a plausible chain of events. In our experiment, vibrational energy is deposited into CH stretching modes or HCH bend overtones and combination bands. Judging from the existing photoelectron spectrum of nitromethane,[60] the most significant coupling between the anionic and the neutral potential energy surfaces will occur involving the nitro wagging mode. The initially deposited energy will eventually drain out of the CH stretching modes because of IVR and is distributed into the rest of the molecular vibrational modes. As a sufficient amount of vibrational energy is redistributed into the modes of the nitro group, excitation of the NO$_2$ wagging modes (calculated to be on the order of 350−450 cm^{-1} for the molecules under study) facilitates near-resonant passage onto the neutral potential energy surface, that is, electron emission.[13,60] We stress that, although this seems to be a likely relaxation mechanism, we cannot rule out other, nonstatistical relaxation pathways that would couple the CH stretching motion directly to the electron-loss channel.

The time and frequency resolution of our experiment currently does not afford statements on the time scale of IVR or of autodetachment. Just as the reverse process to VAD, namely, the accommodation of an excess electron into the highest occupied molecular orbital of a nitroalkane by electron attachment, VAD is a result of the breakdown of the Born−Oppenheimer approximation as the potential energy curves of the anion and the neutral species cross.[78,79] The time constant of the autodetachment process itself from a state with sufficiently populated NO$_2$ wagging modes will be very short.[79] However, it is conceivable that the time for electron emission can be much longer than the time for thermalization, because sufficient energy must be pooled in the emission-active modes.

We note that Dlott and co-workers have observed energy redistribution in liquid nitromethane from the CH stretching modes into the NO$_2$ wagging modes on the order of tens of picoseconds in time-resolved IR pump/Raman probe spectroscopy.[80,81] Another mechanism of vibrational energy transport that has been observed by the same group in ultrafast thermal flash experiments is the near-ballistic flow of energy through alkane chains, made feasible by the excitation of modes that are delocalized over the molecular frame.[82] On the time scale of our experiment (tens of microseconds), we are not able to see any effect of the chain length on the autodetachment efficiency of the excited nitroalkanes. Given that efficient energy transfer from the methyl group to the nitro group has been observed in liquid nitromethane to take on the order of tens of picoseconds and that even an increase of an order of magnitude per CH_2 group would leave us at a time scale of $\sim 10^{-7}$ s, we judge that size effects make virtually no difference for the molecules under study in the present experiment. Time-resolved ultrafast infrared-pump/visible-probe photoelectron spectroscopy would be a good method to further investigate the details of the coupling time scale.

5. Summary, Conclusions, and Outlook

We have performed vibrational spectroscopy in the CH stretching region of nitroalkane anions by Ar-PD and electron autodetachment. Our data show that electron autodetachment upon absorption of one IR photon exciting the fundamental of a CH stretching vibration is feasible for molecules at least up to the size of nitropentane. For the smaller molecules, we can assign the transitions seen in the spectra to the CH stretching fundamentals and their Fermi resonances with overtones and combination bands of HCH bending modes for the lowest-energy isomers. We offer possible explanations for the relaxation mechanism that ultimately leads to electron autodetachment. A closer look at the details of the coupling mechanism between the initially excited CH stretching modes and electron detachment, for example, by using time-resolved photoelectron spectroscopy, is certainly warranted to help us better understand this aspect of VAD.

Acknowledgment. We thank Professor Kit H. Bowen for providing us with a photoelectron spectrum of nitroethane prior to publication. We also thank Professor G. Barney Ellison for helpful discussions. We acknowledge support from the Atomic, Molecular, and Optical Physics Division of the National Science Foundation through the JILA Physics Frontier Center (NSF Grant PHY-0551010) and from the donors of the Petroleum Research Fund of the American Chemical Society. J.F.S. acknowledges financial support from the National Science Foundation (CHE-0710146) and the Division of Basic Energy Sciences, US Department of Energy (DE-FG02-07ER15884). Michael Harding (Mainz) is thanked for performing some calculations.

Supporting Information Available: This material is available free of charge via the Internet at http://pubs.acs.org.

References and Notes

(1) Oomens, J.; van Roij, A. J. A.; Meijer, G.; von Helden, G. *Astrophys. J.* **2000**, *542*, 404.
(2) Heijnsbergen, D.; Duncan, M. A.; Meijer, G.; von Helden, G. *Chem. Phys. Lett.* **2001**, *349*, 220.
(3) Oomens, J.; Meijer, G.; von Helden, G. *J. Phys. Chem. A* **2001**, *105*, 8302.
(4) van Heijnsbergen, D.; Jaeger, T. D.; von Helden, G.; Meijer, G.; Duncan, M. A. *Chem. Phys. Lett.* **2002**, *364*, 345.
(5) van Heijnsbergen, D.; von Helden, G.; Meijer, G.; Maitre, P.; Duncan, M. A. *J. Am. Chem. Soc.* **2002**, *124*, 1562.
(6) Jaeger, T. D.; van Heijnsbergen, D.; Klippenstein, S. J.; von Helden, G.; Meijer, G.; Duncan, M. A. *J. Am. Chem. Soc.* **2004**, *126*, 10981.
(7) Kapota, C.; Lemaire, J.; Maitre, P.; Ohanessian, G. *J. Am. Chem. Soc.* **2004**, *126*, 1836.
(8) Fridgen, T. D.; MacAleese, L.; McMahon, T. B.; Lemaire, J.; Maitre, P. *Phys. Chem. Chem. Phys.* **2006**, *8*, 955.
(9) Bailey, C. G.; Kim, J.; Dessent, C. E. H.; Johnson, M. A. *Chem. Phys. Lett.* **1997**, *269*, 122.
(10) Ayotte, P.; Bailey, C. G.; Kim, J.; Johnson, M. A. *J. Chem. Phys.* **1998**, *108*, 444.
(11) Ayotte, P.; Weddle, G. H.; Kim, J.; Johnson, M. A. *Chem. Phys.* **1998**, *239*, 485.
(12) Weber, J. M.; Kelley, J. A.; Nielsen, S. B.; Ayotte, P.; Johnson, M. A. *Science* **2000**, *287*, 2461.
(13) Weber, J. M.; Robertson, W. H.; Johnson, M. A. *J. Chem. Phys.* **2001**, *115*, 10718.
(14) Kelley, J. A.; Robertson, W. H.; Johnson, M. A. *Chem. Phys. Lett.* **2002**, *362*, 255.
(15) Robertson, W. H.; Johnson, M. A. *Annu. Rev. Phys. Chem.* **2003**, *54*, 173.
(16) Diken, E. G.; Weddle, G. H.; Headrick, J. M.; Weber, J. M.; Johnson, M. A. *J. Phys. Chem. A* **2004**, *108*, 10116.
(17) Weber, J. M.; Schneider, H. *J. Chem. Phys.* **2004**, *120*, 10056.
(18) Schneider, H.; Boese, A. D.; Weber, J. M. *J. Chem. Phys.* **2005**, *123*, 084307.
(19) Schneider, H.; Vogelhuber, K. M.; Schinle, F.; Weber, J. M. *J. Am. Chem. Soc.* **2007**, *129*, 13022.
(20) Schneider, H.; Vogelhuber, K. M.; Weber, J. M. *J. Chem. Phys.* **2007**, *127*, 114311.
(21) Schneider, H.; Weber, J. M. *J. Chem. Phys.* **2007**, *127*, 244310.
(22) Schneider, H.; Weber, J. M.; Myshakin, E. M.; Jordan, K. D.; Bopp, J. C.; Herden, T.; Johnson, M. A. *J. Chem. Phys.* **2007**, *127*, 084319.
(23) Bieske, E. J. *Chem. Soc. Rev.* **2003**, *32*, 231.
(24) Wild, D. A.; Bieske, E. J. *Int. Rev. Phys. Chem.* **2003**, *22*, 129.
(25) Wild, D. A.; Loh, Z. M.; Wilson, R. L.; Bieske, E. J. *Chem. Phys. Lett.* **2003**, *369*, 684.
(26) Thompson, C. D.; Poad, B. L. J.; Emmeluth, C.; Bieske, E. J. *Chem. Phys. Lett.* **2006**, *428*, 18.
(27) Bieske, E. J.; Dopfer, O. *Chem. Rev.* **2000**, *100*, 3963.
(28) Dopfer, O. *Int. Rev. Phys. Chem.* **2003**, *22*, 437.
(29) Gregoire, G.; Velasquez, J.; Duncan, M. A. *Chem. Phys. Lett.* **2001**, *349*, 451.
(30) Gregoire, G.; Brinkmann, N. R.; van Heijnsbergen, D.; Schaefer, H. F.; Duncan, M. A. *J. Phys. Chem. A* **2003**, *107*, 218.
(31) Walters, R. S.; Brinkmann, N. R.; Schaefer, H. F.; Duncan, M. A. *J. Phys. Chem. A* **2003**, *107*, 7396.
(32) Jaeger, J. B.; Jaeger, T. D.; Brinkmann, N. R.; Schaefer, H. F.; Duncan, M. A. *Can. J. Chem.* **2004**, *82*, 934.
(33) Walters, R. S.; Duncan, M. A. *Aust. J. Chem.* **2004**, *57*, 1145.
(34) Douberly, G. E.; Ricks, A. M.; Ticknor, B. W.; McKee, W. C.; Schleyer, P. V. R.; Duncan, M. A. *J. Phys. Chem. A* **2008**, *112*, 1897.
(35) Douberly, G. E.; Ricks, A. M.; Ticknor, B. W.; Schleyer, P. V. R.; Duncan, M. A. *J. Am. Chem. Soc.* **2007**, *129*, 13782.
(36) Kasalova, V.; Allen, W. D.; Schaefer, H. F.; Pillai, E. D.; Duncan, M. A. *J. Phys. Chem. A* **2007**, *111*, 7599.
(37) Walker, N. R.; Walters, R. S.; Tsai, M. K.; Jordan, K. D.; Duncan, M. A. *J. Phys. Chem. A* **2005**, *109*, 7057.
(38) Crim, F. F. *Annu. Rev. Phys. Chem.* **1993**, *44*, 397.
(39) Lehmann, K. K.; Scoles, G.; Pate, B. H. *Annu. Rev. Phys. Chem.* **1994**, *45*, 241.
(40) Nesbitt, D. J.; Field, R. W. *J. Phys. Chem.* **1996**, *100*, 12735.
(41) Boyall, D.; Reid, K. L. *Chem. Soc. Rev.* **1997**, *26*, 223.
(42) Ueba, H. *Prog. Surf. Sci.* **1997**, *55*, 115.
(43) Gruebele, M.; Bigwood, R. *Int. Rev. Phys. Chem.* **1998**, *17*, 91.
(44) Keske, J. C.; Pate, B. H. *Annu. Rev. Phys. Chem.* **2000**, *51*, 323.
(45) Assmann, J.; Kling, M.; Abel, B. *Angew. Chem., Int. Ed.* **2003**, *42*, 2226.
(46) Stolow, A. *Int. Rev. Phys. Chem.* **2003**, *22*, 377.
(47) Sanov, A.; Lineberger, W. C. *Phys. Chem. Chem. Phys.* **2004**, *6*, 2018.
(48) Yoo, H. S.; DeWitt, M. J.; Pate, B. H. *J. Phys. Chem. A* **2004**, *108*, 1348.
(49) Yoo, H. S.; DeWitt, M. J.; Pate, B. H. *J. Phys. Chem. A* **2004**, *108*, 1365.
(50) Yoo, H. S.; McWhorter, D. A.; Pate, B. H. *J. Phys. Chem. A* **2004**, *108*, 1380.
(51) Carpenter, B. K. *Annu. Rev. Phys. Chem.* **2005**, *56*, 57.
(52) Chakraborty, A.; Seth, D.; Setua, P.; Sarkar, N. *J. Phys. Chem. B* **2006**, *110*, 5359.
(53) Elles, C. G.; Crim, F. F. *Annu. Rev. Phys. Chem.* **2006**, *57*, 273.
(54) Giese, K.; Petkovic, M.; Naundorf, H.; Kuhn, O. *Phys. Rep.* **2006**, *430*, 211.
(55) Hertel, I. V.; Radloff, W. *Rep. Prog. Phys.* **2006**, *69*, 1897.
(56) Leitner, D. M.; Havenith, M.; Gruebele, M. *Int. Rev. Phys. Chem.* **2006**, *25*, 553.
(57) Richardson, O. W. *The Emission of Electricity from Hot Bodies*; Longmans Green and Company: London, 1921.
(58) Neumark, D. M.; Lykke, K. R.; Andersen, T.; Lineberger, W. C. *J. Chem. Phys.* **1985**, *83*, 4364.
(59) Maeyama, T.; Yagi, I.; Murota, Y.; Fujii, A.; Mikami, N. *J. Phys. Chem. A* **2006**, *110*, 13712.

(60) Compton, R. N.; Carman, H. S.; Desfrancois, C.; AbdoulCarmine, H.; Schermann, J. P.; Hendricks, J. H.; Lyapustina, S. A.; Bowen, K. H. *J. Chem. Phys.* **1996**, *105*, 3472.

(61) Parr, R. G.; Yang, W. *Density-Functional Theory of Atoms and Molecules*; Oxford University Press: New York, 1989.

(62) Becke, A. D. *Phys. Rev. A* **1988**, *38*, 3098.

(63) Lee, C. T.; Yang, W. T.; Parr, R. G. *Phys. Rev. B* **1988**, *37*, 785.

(64) Weigend, F.; Häser, M. *Theor. Chem. Acc.* **1997**, *97*, 331.

(65) Weigend, F.; Häser, M.; Patzelt, H.; Ahlrichs, R. *Chem. Phys. Lett.* **1998**, *294*, 143.

(66) Ahlrichs, R.; Bär, M.; Häser, M.; Horn, H.; Kölmel, C. *Chem. Phys. Lett.* **1989**, *162*, 165.

(67) Schäfer, A.; Huber, C.; Ahlrichs, R. *J. Chem. Phys.* **1994**, *100*, 5829.

(68) Raghavachari, K.; Trucks, G. W.; Pople, J. A.; Head-Gordon, M. *Chem. Phys. Lett.* **1989**, *157*, 479.

(69) Almlöf, J.; Taylor, P. R. *J. Chem. Phys.* **1987**, *86*, 4070.

(70) Mills, I. M. In *Modern Spectroscopy: Modern Research*; Rao, K. N., Matthews, C. W., Eds.; Academic Press: New York, 1972; pp 115.

(71) Stanton, J. F.; Lopreore, C. L.; Gauss, J. *J. Chem. Phys.* **1998**, *108*, 7190.

(72) Gauss, J.; Stanton, J. F. *Chem. Phys. Lett.* **1997**, *276*, 70.

(73) Stanton J. F. and the integral packages MOLECULE (Almlöf, J.; Taylor, P. R.), PROPS (Taylor, P. R.), and ABACUS (Helgaker, T.; Jensen, H. J. Aa.; Jørgensen, P.; Olsen, J.). For the current version, see http://www.aces2.de. ACES II.

(74) Stanton, J. F.; Gauss, J.; Watts, J. D.; Lauderdale, W. J.; Bartlett, R. J. *Int. J. Quantum Chem. Symp.* **1992**, *26*, 879.

(75) Matthews, D. A.; Vazquez J.; Stanton, J. F. GUINEA, a program for numerical vibrational Rayleigh-Schrödinger perturbation calculations. 2008.

(76) Stanton, J. F.; Ware, A. F.; Flowers, B. A.; Ellison, G. B. *J. Mol. Spec.* **2008**, In Press.

(77) Bowen, K. H.

(78) Gutsev, G. L.; Bartlett, R. J. *J. Chem. Phys.* **1996**, *105*, 8785.

(79) Sommerfeld, T. *Phys. Chem. Chem. Phys.* **2002**, *4*, 2511.

(80) Hong, X. Y.; Chen, S.; Dlott, D. D. *J. Phys. Chem.* **1995**, *99*, 9102.

(81) Shigeto, S.; Pang, Y.; Fang, Y.; Dlott, D. D. *J. Phys. Chem. B* **2008**, *112*, 232.

(82) Wang, Z. H.; Carter, J. A.; Lagutchev, A.; Koh, Y. K.; Seong, N. H.; Cahill, D. G.; Dlott, D. D. *Science* **2007**, *317*, 787.

JP800124S